King Saud University

Arabian Journal of Chemistry

ORIGINAL ARTICLE

Polycyclic aromatic hydrocarbon-bridged coumarin derivatives for organic light-emitting devices

Yanmei Li [a], Tianzhi Yu [a,*], Wenming Su [b,*], Youjia Wang [a], Yuling Zhao [c], Hui Zhang [a]

[a] *Key Laboratory of Opto-Electronic Technology and Intelligent Control (Ministry of Education), Lanzhou Jiaotong University, Lanzhou 730070, China*
[b] *Printable Electronics Research Center, Suzhou Institute of Nano-Tech and Nano-Bionics, Chinese Academy of Sciences, Suzhou 215123, China*
[c] *School of Chemical and Biological Engineering, Lanzhou Jiaotong University, Lanzhou 730070, China*

Abstract   Three biscoumarin dyes bridged by polycyclic aromatic bridges (anthracen, pyrene and dibenzo[*g,p*]chrysene) were prepared as the emissive materials for the application of organic light-emitting devices. The relationship between their structures, photophysical properties, electrochemical properties and performances of organic light-emitting devices are described. The multilayered doped devices with a configuration of ITO/NPB (20 nm)/TBADN: biscoumarin compound (x wt%, 30 nm)/TPBi (30 nm)/Liq (2 nm)/Al (100 nm) have been successfully fabricated by vacuum-deposition method. All the devices showed green emission with high electroluminescent efficiencies. Especially, the device based on the compound containing pyrene as a bridge group at 7% doping concentration showed the best performance with a maximum brightness of 10552 cd/m^2, maximum luminous efficiency of 5.39 cd/A and maximum external quantum efficiency (EQE) of 2.35%.

1. Introduction

Recently, polycyclic aromatic hydrocarbons (PAHs), such as anthracen, pyrene, perylene and chrysene, have been used widespreadly in molecular electronics, optoelectronics, energy conversion devices and various other forms of nanotechnology due to their chemical stabilities and photochemical properties (Watson et al., 2001; Mishra and Buerle, 2012; Itoh, 2012; Forrest and Thompson, 2007; van de Craats et al., 1999; van de Craats et al., 2003). Furthermore, PAHs are the representative building blocks for fluorescent materials because of their excellent stability, strong photoluminescence (PL) and easy chemical modification. Branched π-conjugated and dendritic compounds with anthracene, pyrene, fluorene and chrysene as cores have been prepared for possible application in organic solar cells, light-emitting devices and non-linear optical devices

Production and hosting by Elsevier

(Kim et al., 2013; Heyer and Ziessel, 2013; Teng et al., 2010; Lin et al., 2018; Detert et al., 2010; Kanibolotsky et al., 2010). PAHs have planar π-conjugated skeleton, which could increase the π-electron delocalization and charge transport of the final materials, and could broaden absorption of the materials. However, the rigid and planar structure make PAHs ready to form close π-π stacking, leading to severe PL quenching by aggregation, which reduce electroluminescence (EL) efficiency and degrade color purity. How to control the molecular packing of aromatic compounds in solid state is an essential issue for scientists. Many researchers attempted to resolve these problems by grafting bulky groups to the PAHs skeleton. For example, bulky substituents at 9,10-positions of anthracene ring are often used to restrain the aggregation between molecules in the solid state, yielding an amorphous compounds with efficient blue electroluminescence (Shi and Tang, 2002; Zhang et al., 2003; Liu et al., 2003; Kim et al., 2009). So far, many blue emitters with anthracene and pyrene as the single cores or side moieties have been investigated for OLEDs since they have high PL efficiencies (Park et al., 2012; Lai et al., 2011; Gong et al., 2010; Figueira-Duarte et al., 2010). Dibenzochrysene (DBC), a twisted polycyclic aromatic hydrocarbon, and its derivatives have attracted tremendous attention because of their outstanding photophysical properties are similar to those of fluorene, pyrene and perylene (Navale et al., 2011; Suzuki et al., 2015; Heyer and Ziessel, 2013; Zhang et al., 2017). Heyer el al. introduced a diketopyrrolopyrrole (DPP) or borondipyrromethene (Bodipy) unit into the dibenzochrysene core to promote functionalization and provided evidence of very efficient intramolecular cascade energy transfer (Heyer and Ziessel, 2013). In order to weaken the intermolecular interactions between molecules and prevent the self-quenching of fluorescence in solid state resulted from the planar structure of dibenzochrysene core, Jeong et al. incorporated the bulky *tert*-butyl substituents and diphenylamine moieties into the dibenzochrysene core to obtain blue materials and the doped devices showed highly efficient blue emission with an external quantum efficiency (EQE) of 4.72% at 20 mA/cm^2 (Jeong et al., 2017). The double-layer OLEDs based the dibenzochrysene derivatives with four aromatic amino substituents showed blue-green emission with a high luminous efficiency of 3.2 lm/W and a high quantum efficiency of 2% at a luminance of 300 cd/m^2 (Tokito et al., 2000). Recently, Liu et al. used the dibenzochrysene derivatives with four phenyls as the host materials in a red phosphorescent OLEDs, and the device exhibited decent electroluminescence with a maximum EQE of 14.4% (Liu et al., 2017).

Coumarin derivatives attracted tremendous attentions because of their applications in laser dyes, fluorescent dyes and so on (Haugland, 1994–1996.; Schwander et al., 1988; Wolfbeis et al., 1985; Tripathy and Bisht, 2006; Gilat et al., 1999; Kitamura et al., 2007; Hara et al., 2001). Their photophysical properties are strongly dependent on the nature and the position of substituents and also on the rigidity of the molecules (Ammar et al., 2003; Azuma et al., 2003; Yu et al., 2007; Yu et al., 2006). The coumarin derivatives with electron donating groups at the 7-position exhibit strong fluorescence in blue-green region, but the coumarin derivatives as emissive materials in OLEDs are easily self-quenched in solid state due to intermolecular interaction and aggregation. Therefore, they are always doped in a variety of host materials to fabricate OLEDs with reasonable luminous efficiencies, and the doping
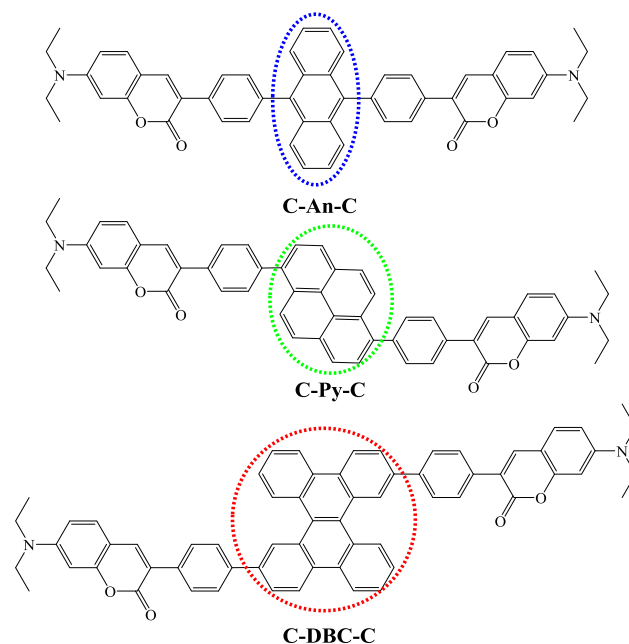

Fig. 1 Chemical structures of synthesized PAHs-based biscoumarin derivatives.

concentration is very low (Yu et al., 2010; Zhang et al., 2010; Zhang et al., 2017; Yu et al., 2017).

As a part of our continuous researches in developing new coumarin derivatives for OLEDs, in this study, three PAHs-based biscoumarin derivatives were prepared for OLEDs in order to investigate their photophysical features and electroluminescence properties, and to find out possible structure–property relationships, in which anthracen, pyrene and dibenzo[g,p] chrysene cores are used as π-conjugations to space two 7-diethylamino-coumarin luminophores (Fig. 1).

2. Experimental

2.1. Materials and methods

2-Bromo-9-fluorenone was obtained from Energy Chemical (China). All the other chemicals were analytical grade reagent.

7-(Diethylamino)-3-(4-(4,4,5,5-tetramethyl-1,3,2-dioxaborolan-2-yl)phenyl)coumarin and 9,10-dibromoanthracene were prepared according to the literatures (Yu et al., 2017; Luo et al., 2018). 3,3′-(Anthracene-9,10-diylbis(4,1-phenylene))bis(7-(diethylamino)-2H-chromen-2-one) (**C-An-C**) and 3,3′-(pyrene-1,6-diylbis(4,1-phenylene))bis(7-(diethylamino)-2H-chromen-2-one) (**C-Py-C**) were synthesized according to the literature (Zhang et al., 2018).

All instruments used to characterize the structures, photophysical and electrochemical properties of the compounds were described in our previous paper (Li et al., 2019).

2.2. Synthesis and characterization of the compound C-DBC-C

2.2.1. 3,11-Dibromodibenzo[g,p]chrysene

2-bromo-9-fluorenone (2.0 g, 7.72 mmol), zinc powder (9.19 g, 140.5 mmol) and zinc chloride (1.89 g, 13.9 mmol) were

dissolved in 50% aqueous THF (60 mL), and the reaction mixture was stirred at 25 °C for 3 h. Then, 5 mL of 3 N HCl was added in the reaction mixture, and the Zn powder was removed by filtering. The filtrate was extracted with dichloromethane (3 × 50 mL). The combined organic phase was washed with water (3 × 50 mL) and brine (3 × 50 mL), and dried over anhydrous Na_2SO_4. After filtration and evaporation of the solvent in vacuum, the crude pinacol was used in the next step without further purification.

The foregoing pinacol was dissolved in AcOH (50 mL) and concentrated HCl (5 mL), and the mixture was stirred overnight at 110 °C. After cooling to room temperature, it was filtered and washed with absolute ethyl alcohol and dichloromethane. The crude was purified by chromatography on silica gel using petroleum ether/dichloromethane (5:2, v/v) as the eluent to give yellow powder (1.0 g, 53.3%). m.p. 205–207 °C. ^{1}H NMR (500 MHz, CDCl$_3$, δ, ppm): 8.07 (m, 3H, Ar-H), 7.90 (dd, J = 8.6 Hz, 1H, Ar-H), 7.76 (d, J = 7.6 Hz, 1H, Ar-H), 7.67 (d, J = 8.1 Hz, 1H, Ar-H), 7.55 (dd, J = 8.1 Hz, 1H, Ar-H), 7.39 (t, J = 7.6 Hz, 2H, Ar-H), 7.18 (m, 2H, Ar-H), 7.13 (t, J = 7.6 Hz, 1H, Ar-H), 6.96 (d, J = 7.7 Hz, 1H, Ar-H), 6.60 (d, J = 7.8 Hz, 1H, Ar-H).

2.2.2. 3,3′-(Dibenzo[g,p]chrysene-3,11-diylbis(4,1-phenylene)) bis(7-(diethylamino)coumarin (C-DBC-C)

The mixture of 3,11-dibromodibenzo[g,p]chrysene (1.20 g, 2.47 mmol), 7-(diethylamino)-3-(4-(4,4,5,5-tetramethyl-1,3,2-d ioxaborolan-2-yl)phenyl)coumarin (2.60 g, 6.20 mmol), Pd (PPh$_3$)$_4$ (0.0.30 g, 0.26 mmol), TBAB (0.08 g, 0.25 mmol) and Na$_2$CO$_3$ (0.60 g, 15 mml) was dissolved in absolute toluene (150 mL) under nitrogen atmosphere. The suspension was heated up to 120 °C and stirred vigorously. After 10 min, distilled water 3.7 (mL) was added. The reaction solution was stirred at 110 °C for 20 h. After the reaction solution was cooled to room temperature, the solvent was evaporated in vacuum, and the mixture was dissolved in dichloromethane (150 mL) and washed with water (3 × 100 mL). The organic phase was dried over anhydrous Na$_2$SO$_4$ and concentrated in vacuum. The crude product was purified by column chromatography using ethyl acetate/dichloromethane/petroleum ether (1/4/10, v/v/v) as the eluent to afford **C-DBC-C** as yellow powder (1.45 g, 64.5%). m.p. >250 °C. ^{1}H NMR (500 MHz, CDCl$_3$, δ, ppm): 8.32–8.28 (m, 2H), 8.15 (d, J = 7.8 Hz, 1H), 8.09 (d, J = 8.4 Hz, 1H), 7.88 (d, J = 8.0 Hz, 1H), 7.85–7.80 (m, 3H), 7.77–7.28 (m, 3H), 7.69 (t, J = 8.5 Hz, 4H), 7.49 (d, J = 8.4 Hz, 2H), 7.44–7.37 (m, 2H), 7.35–7.28 (m, 3H), 7.20 (t, J = 7.6 Hz, 1H), 7.11 (t, J = 7.5 Hz, 2H), 6.70 (d, J = 7.9 Hz, 1H), 6.59(t, J = 9.0 Hz, 2H), 6.53 (d, J = 10.0 Hz, 2H), 3.47–3.37 (m, 8H), 1.22 (dd, J = 7.0, 7.0 Hz, 12H). ^{13}C NMR (151 MHz, CDCl$_3$, δ, ppm): 197.1,

161.6, 156.2, 150.6, 141.3, 141.0, 140.6, 140.5, 140.4, 140.3, 140.1, 139.2, 138.5, 137.0, 135.5 (s), 134.8, 133.2, 130.4, 130.2, 129.3, 129.0 128.9, 128.7, 128.4, 128.2, 128.1, 127.9, 127.4, 126.9, 126.8, 126.6, 124.7, 124.1, 124.0, 123.4, 120.8, 120.6, 120.3, 120.1, 109.1, 109.0, 108.9, 97.1, 68.7 (s), 44.9, 12.4. HRMS: Calcd. for C$_{64}$H$_{50}$N$_2$O$_4$, 949.3408 [M + K]; Found: 949.3458. Anal.Calcd. for C$_{64}$H$_{50}$N$_2$O$_4$ (%): C, 84.37, H, 5.53, N, 3.07. Found: C, 84.45, H, 5.49, N, 3.09.

## 3. Results and discussion

3.1. Synthesis and characterization

Three compounds (**C-An-C**, **C-Py-C** and **C-DBC-C**) based on the polycyclic aromatic (anthracen, pyrene and dibenzo[g,p] chrysene) cores and 7-diethylamino-coumarin moiety were designed and synthesized from the Suzuki cross-coupling reactions of the corresponding dibrominated polycyclic aromatic compounds with the coumarin arylboronic ester. The compounds **C-An-C** and **C-Py-C** were prepared by methods described in our previous article (Zhang et al., 2018). The synthetic routes of the compound **C-DBC-C** are shown in Scheme 1. The key step is the formation of the 3,11-dibromodibenzo[g,p]chrysene as the twisted core, which underwent the acid-catalyzed dehydration/cyclization to the intermediate through a pinacol rearrangement, as reported by Klumpp et al. (Klumpp et al., 1997) Then, the target compound **C-DBC-C** was synthesized by the Suzuki cross-coupling reaction of 3,11-dibromodibenzo[g,p]chrysene with the coumarin arylboronic ester as yellow solid with moderate yield (64.5%) after purification by column chromatography and characterized by ^{1}H NMR, ^{13}C NMR, HRMS and elemental analysis.

3.2. Photophysical, electrochemical and thermal properties of the compounds

The measurements of UV–vis absorption and photoluminescence spectra of the compounds were done in the air at room temperature. The UV–vis absorption and photoluminescence spectra of the compounds in chloroform solutions are shown in Fig. 2, and their photophysical data are summarized in Table 1.

The absorption spectra of the compounds **C-An-C** and **C-Py-C** in chloroform solutions are similar, exhibiting a relatively weak absorption band at 275 nm for **C-An-C** and 282 nm for **C-Py-C** in high energy region and a strong absorption band at 412 nm in low energy region. The former absorption band is attributed to the π → π* transition of the
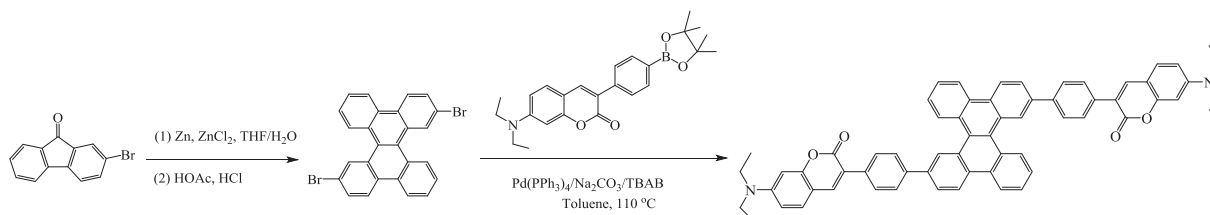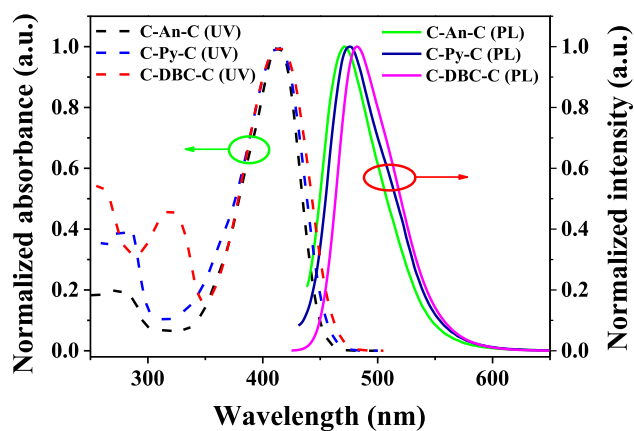

Scheme 1   Synthetic route to the compound **C-DBC-C**.

Fig. 2 UV–vis absorption and photoluminescence spectra of the compounds in chloroform solutions (C = 1.0 × 10⁻⁵ mol/L, λ_{ex} = 412 nm).

conjugative polycyclic aromatic cores, while the latter absorption band can be assigned to the $\pi \rightarrow \pi^*$ transition of the 7-diethylamino-coumarin moieties. The absorption spectrum of the compound **C-DBC-C** also exhibits two absorption bands at 319 and 412 nm, which are attributed to the $\pi \rightarrow \pi^*$ transition of dibenzo[g,p]chrysene core and the $\pi \rightarrow \pi^*$ transition of the 7-diethylamino-coumarin moieties, respectively. It can be seen that the absorption band of the compounds in high energy region is red-shifted from anthracene to dibenzo[g,p]chrysene with the increase of conjugation degree of polycyclic aromatic cores. As shown in Fig. 2, under excitation at the absorption band maximum (410 nm), in chloroform solutions, the compounds exhibit strong blue-green emissions with the maximum peaks at 472, 475 and 482 nm, respectively. It was found that, from anthracene to dibenzo[g,p]chrysene, the emission peak was red-shifted due to the increase of conjugation degree of the molecules and their Stokes shifts are ca. 3085, 3219 and 3525 cm⁻¹, respectively.

In addition, the fluorescence quantum yields (Φ_f) and decay lifetimes (τ) of the compounds in chloroform solutions were measured at room temperature. The fluorescence quantum yields of **C-An-C**, **C-Py-C** and **C-DBC-C** were measured to be 86.32, 89.31 and 87.53%, and their fluorescence decay lifetimes were measured to be 8.90, 8.46 and 12.50 ns. They all belong to the fluorescence nature of the emission.

The electrochemical properties of **C-An-C**, **C-Py-C** and **C-DBC-C** were investigated by cyclic voltammetry (CV). The cyclic voltammograms and HOMO and LUMO energy levels of **C-An-C** and **C-Py-C** were reported in our previous article (Zhang et al., 2018). The cyclic voltammogram of **C-DBC-C** is shown in Fig. 3. The first oxidation potential of **C-DBC-C** was at ca. 0.53 V. At the same condition, the Fc/Fc⁺ potential were measured to be 0.26 V. Thus, the HOMO energy level of
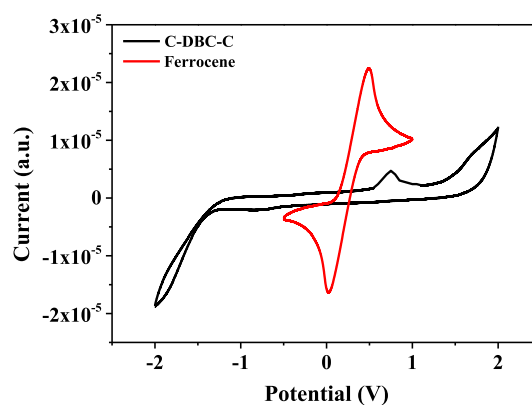

Fig. 3 Cyclic voltammograms of **C-DBC-C** and ferrocene (Scan rate: 10 mV/s; solvent: chloroform).

C-DBC-C was calculated to be −5.07 eV regarding the energy level of ferrocene/ferrocenium as −4.80 eV (Cardona et al., 2011). From its UV–vis absorption spectrum, the optical band edge of the compound was estimated to be ca. 471 nm, which corresponds to 2.63 eV. Then, the LUMO energy level of **C-DBC-C** was calculated to be −2.44 eV.

The thermal stabilities of **C-An-C**, **C-Py-C** and **C-DBC-C** were investigated by thermal gravimetric analysis (TGA) measurements under nitrogen atmosphere. The TGA curves and the decomposition temperatures of **C-An-C** and **C-Py-C** were reported in our previous article (Zhang et al., 2018). The TGA curve of **C-DBC-C** is shown in Fig. 4. With increasing temperature, the compound **C-DBC-C** exhibits good thermal stability up to 436 °C (< 1% weight loss). At 436 °C, there is a sharp weight loss in its TGA curve, indicating that the compound **C-DBC-C** undergoes one large-stage decomposition process.

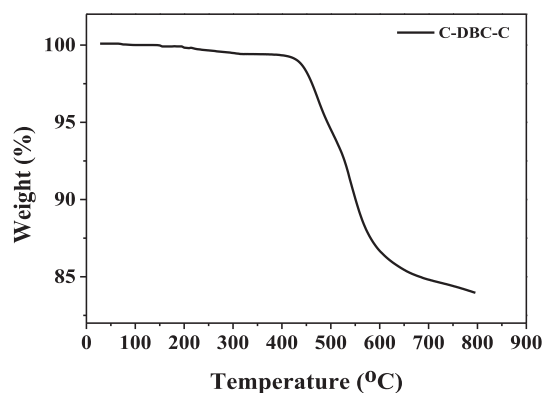**Fig. 4** Thermogravimetric analysis (TGA) of **C-DBC-C** in nitrogen atmosphere (heating rate: 10 °C/min).

Table 1 Photophysical, thermal and electrochemical properties of **C-An-C**, **C-Py-C** and **C-DBC-C**.

Compound	UV–vis (nm)	PL (nm)	T_d (°C)	Φ_f (%)	τ (ns)	HOMO (eV)	LUMO (eV)	E_g (eV)
C-An-C	275, 412	472	450	86.32	8.90	−5.10	−2.35	2.75
C-Py-C	282, 412	475	460	89.31	8.46	−5.08	−2.37	2.71
C-DBC-C	319, 412	482	436	87.53	12.50	−5.07	−2.44	2.63

Small organic luminescent materials used in OLEDs should be thermally stable because they are generally deposited onto the appropriate substrate by thermal vacuum deposition technique in the thin amorphous film form or used as blender into a host material. The thermal stability of the luminescent materials has a great influence on the performance of OLEDs because any given amorphous layer will recrystallize slowly as its temperature reaches the glass transition temperature (T_g). Once the material crystallizes, the amorphous film appears pinholes, resulting in the OLEDs does not work properly. Although the glass transition temperatures of **C-An-C**, **C-Py-C** and **C-DBC-C** were not available due to no the instrument of Differential Scanning Calorimeter in our Lab, from their melting points (over than 250 °C) and decomposition temperatures (over than 430 °C), these materials meet with the thermal stability requirement for OLEDs.

In order to visually compare the properties of the compounds, their photophysical, thermal and electrochemical data are listed in Table 1.

3.3. Electroluminescence properties of the compounds

The multilayer OLEDs with a device structure of ITO/NPB (20 nm)/TBADN:Dopant (x wt%, 30 nm)/TPBi (50 nm)/Liq (2 nm)/Al (150 nm) were fabricated by vacuum-processed method as previously described (Li et al., 2019), in which **C-An-C**, **C-Py-C** and **C-DBC-C** were used as dopants. The device structure and the energy diagrams of the materials used in the work are shown in Fig. 5. The device performances (EL spectra, J-V curves, EQE values) were recorded with a Spectra Scan PR655 and a computer controlled Keithley 2400 Sourcemeter.

The characteristics of the OLEDs fabricated with use of **C-An-C**, **C-Py-C** and **C-DBC-C** are shown in Figs. 6–8, and their EL data are summarized in Table 2. The results showed that the performances of the devices fabricated with **C-Py-C** were better than that of **C-An-C** and **C-DBC-C**. As seen in Table 2, the devices based on the compound **C-Py-C** at 7 wt% doping concentration exhibited a maximum brightness of 10552 cd/
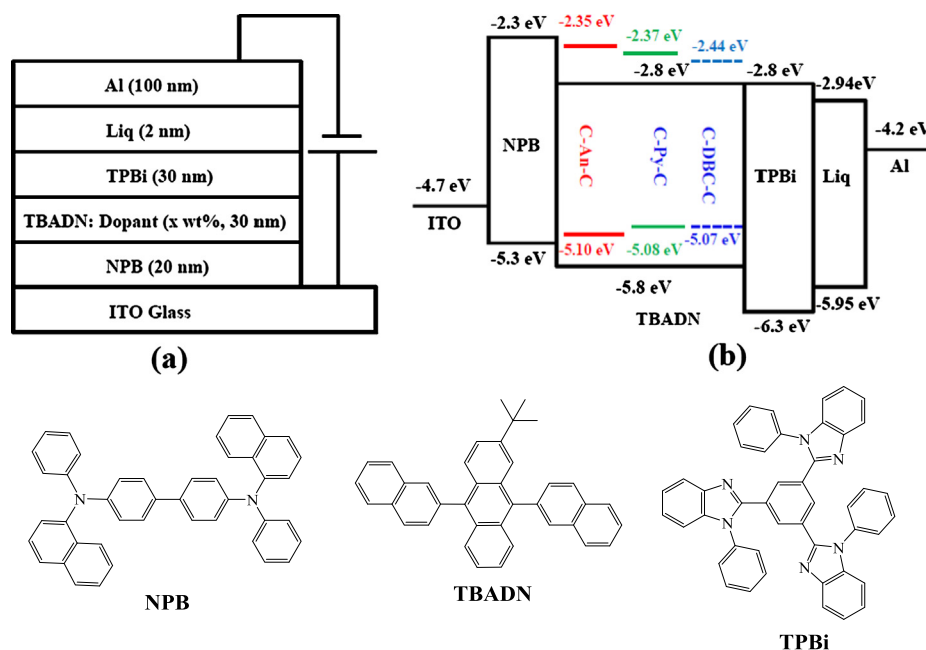

Fig. 5 Schematic diagram of the OLED device configuration (a), the relative HOMO/LUMO energy levels of the materials investigated in this work (b) and structures of NPB, TBADN and TPBi (bottom).
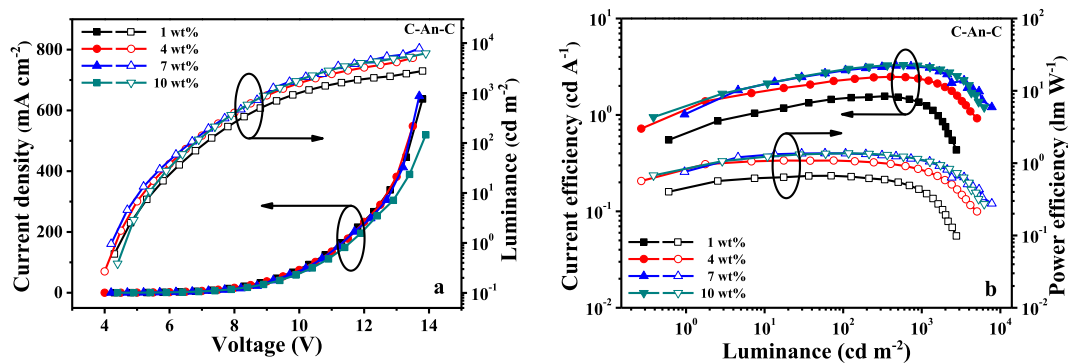

Fig. 6 *I-V-L* characteristics (a) and current/power efficiency *versus* luminance curves (b) for the devices fabricated from **C-An-C** at different dopant concentrations.

Fig. 7 *I-V-L* characteristics (a) and current/power efficiency *versus* luminance curves (b) for the devices fabricated from **C-Py-C** at different dopant concentrations.
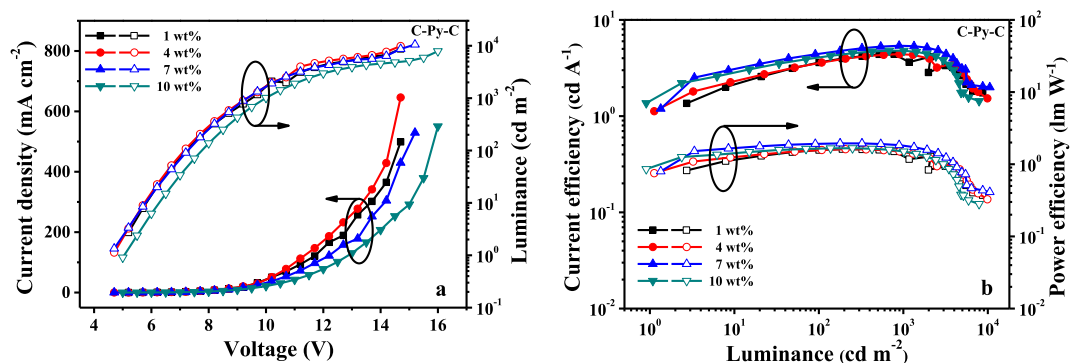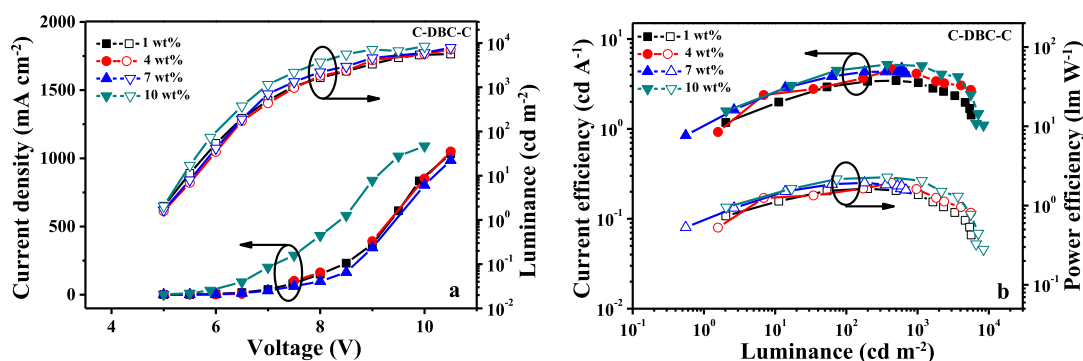

Fig. 8 *I-V-L* characteristics (a) and current/power efficiency *versus* luminance curves (b) for the devices fabricated from **C-DBC-C** at different dopant concentrations.

Table 2 EL performances of **C-An-C**, **C-Py-C** and **C-DBC-C**.

Complex	Concentration	L_{max} (cd/m^2)	LE_{max} (cd/A)	PE_{max} (lm/W)	EQE_{max} (%)
C-An-C	1 wt%	2761	1.57	0.67	1.28
	4 wt%	5056	2.49	1.09	1.59
	7 wt%	7796	3.24	1.37	2.17
	10 wt%	6236	3.29	1.37	1.91
C-Py-C	1 wt%	8707	4.41	1.62	2.18
	4 wt%	9878	4.41	1.62	2.17
	7 wt%	10,552	5.39	1.94	2.35
	10 wt%	7886	4.80	1.67	2.09
C-DBC-C	1 wt%	5658	3.44	1.63	1.65
	4 wt%	7114	4.61	1.93	2.01
	7 wt%	7865	4.73	1.95	2.07
	10 wt%	8433	5.19	2.16	2.13

m^2, maximum luminous efficiencies of 5.39 cd/A and maximum external quantum efficiency (EQE) of 2.35%. At the same doping concentration (7 wt%), the maximum brightness of 7796 cd/m^2, maximum luminous efficiencies of 3.24 cd/A and maximum external quantum efficiency of 2.17% were observed from the devices based on **C-An-C**. As to the compound **C-DBC-C**, the devices with 10 wt% doping concentration showed the maximum brightness of 8433 cd/m^2, maximum luminous efficiencies of 5.19 cd/A and maximum

external quantum efficiency of 2.13%. In comparison with the device performances of the three compounds, the compound **C-Py-C** exhibited better EL performances than **C-An-C** and **C-DBC-C**, which is consistent with their photoluminescence quantum yields.

It was found that the size of polycyclic aromatic core has a great influence on the luminescent properties of the biscoumarin dyes. From anthracene to pyrene, the conjugation degree of the polycyclic aromatic core increases, the
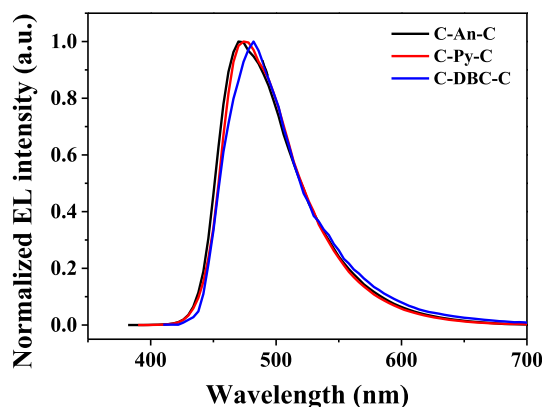
Fig. 9 EL spectra of the devices based on the **C-An-C**, **C-Py-C** and **C-DBC-C** with maximum luminous efficiencies.

photoluminescence quantum yield of the coumarin derivative increases from 86.32% to 89.31%, and the EL performance increases accordingly. When the spacer core is changed to be dibenzo[g,p]chrysene, the conjugation degree of the coumarin derivative increases, but the photoluminescence quantum yield decreases to be 87.53% due to forming close π-π stacking between adjacent molecules, which also reduces the electroluminescence efficiency.

The EL spectra of **C-An-C**, **C-Py-C** and **C-DBC-C** with maximum luminous efficiencies are shown in Fig. 9. Their EL spectra were nearly in accordance with their PL spectra in the solutions, and the devices displayed blue-green emission with the maximum peak at 470, 474 and 481 nm, respectively.

4. Conclusions

In order to investigate the size of polycyclic aromatic hydrocarbons (PAHs) on the luminescent properties of biscoumarin derivatives, three PAHs-based biscoumarin derivatives (**C-An-C**, **C-Py-C** and **C-DBC-C**) were synthesized as the emissive materials for the application of organic light-emitting devices, in which anthracen, pyrene and dibenzo[g,p]chrysene cores were used as π-conjugations to space two 7-diethylamino-coumarin luminophores. The results showed that the size of polycyclic aromatic core has a great influence on the luminescent properties of the biscoumarin dyes, and the compound containing pyrene as bridge group (**C-Py-C**) exhibited better photoluminescence and electroluminescence properties. The vacuum-processed doped devices with a configuration of ITO/NPB (20 nm)/TBADN: biscoumarin compound (x wt%, 30 nm)/TPBi (30 nm)/Liq (2 nm)/Al (100 nm) were fabricated, and the overall performance of devices with **C-Py-C** was higher than the devices with **C-An-C** and **C-DBC-C**. The devices with **C-Py-C** (7 wt%) displayed the best performance with the maximum brightness of 10552 cd/m^2, maximum luminous efficiencies of 5.39 cd/A and maximum external quantum efficiency (EQE) of 2.35%.

Declaration of Competing Interest

There are no conflicts of interest in this article.

References

Ammar, H., Fery-Forgues, S., El Gharbi, R., 2003. UV/vis absorption and fluorescence spectroscopic study of novel symmetrical bis-coumarin dyes. Dyes Pigments 57, 259–265.

Azuma, K., Suzuki, S., Uchiyama, S., Kajiro, T., Santa, T., Imai, K., 2003. A study of the relationship between the chemical structures and the fluorescence quantum yields of coumarins, quinoxalinones and benzoxazinones for the development of sensitive fluorescent derivatization reagents. Photochem. Photobiol. Sci. 2, 443–449.

Cardona, C.M., Li, W., Kaifer, A.E., Stockdale, D., Bazan, G.C., 2011. Electrochemical considerations for determining absolute frontier orbital energy levels of conjugated polymers for solar cell applications. Adv. Mater. 23, 2367–2371.

Detert, H., Lehmann, M., Meier, H., 2010. Star-shaped conjugated systems. Materials 3, 3218–3330.

Figueira-Duarte, T.M., Rosso, P.G.D., Trattnig, R., Sax, S., List, E.J. W., Mullen, K., 2010. Designed suppression of aggregation in polypyrene: Toward high-performance blue-light-emitting diodes. Adv. Mater. 22, 990–993.

S.R. Forrest, M.E. Thompson, Eds. Chem. Rev., 2007, 107, 923-1386 (Special issue on Organic Electronics and Optoelectronics).

Gilat, S.L., Adronov, A., Fréchet, J.M.J., 1999. Light harvesting and energy transfer in novel convergently constructed dendrimers. Angew. Chem. Int. Ed. 38, 1422–1427.

Gong, M.S., Lee, H.S., Jeon, Y.M., 2010. Highly efficient blue OLED based on 9-anthracene-spirobenzofluorene derivatives as host materials. J. Mater. Chem. 20, 10735–10746.

Hara, K., Sayama, K., Ohga, Y., Shinpo, A., Suga, S., Arakawa, H., 2001. A coumarin-derivative dye sensitized nanocrystalline TiO$_2$ solar cell having a high solar-energy conversion efficiency up to 56%. Chem. Commun. 569–570.

Haugland, R.P., 1994–1996. Handbook of Fluorescent Probes and Research Chemicals. Eugene (OR): Molecular Probes.

Heyer, E., Ziessel, R., 2013. Mono-functionalized dibenzo[g, p]-chrysenes for cascade energy transfer. Tetrahedron Lett. 54, 3388–3393.

Itoh, T., 2012. Fluorescence and phosphorescence from higher excited states of organic molecules. Chem. Rev. 112, 4541–4568.

Jeong, S., Kim, S.H., Kim, D.Y., Kim, C., Lee, H.W., Lee, S.E., Kim, Y.K., Yoon, S.S., 2017. Blue organic light-emitting diodes based on diphenylamino dibenzo[g, p]chrysene derivatives. Thin Solid Film 636, 8–14.

Kanibolotsky, A.L., Perepichka, I.F., Skabara, P.J., 2010. Star-shaped π-conjugated oligomers and their applications in organic electronics and photonics. Chem. Soc. Rev. 39, 2695–2728.

Kim, B., Park, Y., Lee, J., Yokoyama, D., Lee, J.-H., Kido, J., Park, J., 2013. Synthesis and electroluminescence properties of highly efficient blue fluorescence emitters using dual core chromophores. J. Mater. Chem. C 1, 432–440.

Kim, S.-K., Yang, B., Park, Y.-I., Ma, Y.G., Lee, J.-Y., Kim, H.-J., Park, J., 2009. Synthesis and electroluminescent properties of highly efficient anthracene derivatives with bulky side groups. Org. Electron. 10, 822–833.

Kitamura, N., Fukagawa, T., Kohtani, S., Kitoh, S.-I., Kunimoto, K.-K., Nakagaki, R., 2007. Synthesis, absorption, and fluorescence properties and crystal structures of 7-aminocoumarin derivatives. J. Photochem. Photobiol. A: Chem. 188, 378–386.

Klumpp, D.A., Baek, D.N., Prakash, G.K.S., Olah, G.A., 1997. Preparation of condensed aromatics by superacidic dehydrative

cyclization of aryl pinacols and epoxides. J. Org. Chem. 62, 6666–6671.

Lai, S.L., Tong, Q.X., Chan, M.Y., Ng, T.W., Lo, M.F., Lee, S.T., Lee, C.S., 2011. Distinct electroluminescent properties of triphenylamine derivatives in blue organic light-emitting devices. J. Mater. Chem. 21, 1206–1211.

Li, X.Y., Tang, P.Y., Yu, T.Z., Su, W.M., Li, Y.M., Wang, Y.J., Zhao, Y.L., Zhang, H., 2019. Two N, N-chelated difluoroboron complexes containing phenanthroimidazole moiety: synthesis and luminescence properties. Dyes Pigments 163, 9–16.

Lin, H.-A., Mitoma, N., Meng, L.K., Segawa, Y., Wakamiya, A., Itami, K., 2018. Hole-transporting materials based on thiophene-fused arenes from sulfur-mediated thienannulations. Mater. Chem. Front. 2, 275–280.

Liu, T.-H., Shen, W.-J., Yen, C.-K., Iou, C.-Y., Chen, H.-H., Banumathy, B., Chen, C.H., 2003. Doped blue emitters of 9,10-di (2-naphthyl)anthracene in organic electroluminescent devices. Syth. Met. 137, 1033–1034.

Liu, X.Y., Tang, X., Zhao, Y., Zhao, D.L., Fan, J., Liao, L.S., 2017. Dibenzo[g, p]chrysene: A new platform for highly efficient red phosphorescent organic light-emitting diodes. Dyes Pigments 146, 234–239.

Luo, Q.L., Zhang, H., Zhao, Y.L., Wang, J., Yu, T.Z., 2018. Synthesis and characterization of 9,10-[di-p-(7-diethylaminocoumarin-3-yl) thiopheneyl]anthracene as fluorescent material. J. Sulfur. Chem. 39, 89–98.

Mishra, A., Buerle, P., 2012. Small molecule organic semiconductors on the move: promises for future solar energy technology. Angew. Chem. Int. Ed. 51, 2020–2067.

Navale, T.S., Thakur, K., Rathore, R., 2011. Sequential oxidative transformation of tetraarylethylenes to 9,10-diarylphenanthrenes and dibenzo/g, p]-chrysenes using DDQ as an oxidant. Org. Lett. 13, 1634–1637.

Park, H., Lee, J., Kang, I., Chu, H.Y., Lee, J.I., Kwon, S.K., Kim, Y.H., 2012. Highly rigid and twisted anthracene derivatives: a strategy for deep blue OLED materials with theoretical limit efficiency. J. Mater. Chem. 22, 2695–2700.

Schwander, H., Hendrix, P., 1988. In: Yamamoto, Y.S. (Ed.), Ullmann's Encyclopedia of Industrial Chemistry, fifth ed., vol. A11, Weinheim, VCH, 1988, p. 280.

Shi, J.M., Tang, C.W., 2002. Anthracene derivatives for stable blue-emitting organic electroluminescence devices. Appl. Phys. Lett. 80, 3201–3203.

Suzuki, N., Fujita, T., Ichikawa, J., 2015. Method for the synthesis of dibenzo[g, p]chrysenes: Domino friedel-crafts-type cyclization of difluoroethenes bearing two biaryl groups. Org. Lett. 17, 4984–4987.

Teng, C., Yang, X.C., Yang, C., Li, S.F., Cheng, M., Hagfeldt, A., Sun, L.C., 2010. Molecular design of anthracene-bridged metal-free organic dyes for efficient dye-sensitized solar cells. J. Phys. Chem. C 114, 9101–9110.

Tokito, S., Noda, K., Fujikawa, H., Taga, Y., 2000. Highly efficient blue-green emission from organic light-emitting diodes using dibenzochrysene derivatives. Appl. Phys. Lett. 77, 160–162.

Tripathy, U., Bisht, P.B., 2006. Effect of donor-acceptor interaction strength on excitation energy migration and diffusion at high donor concentrations. J. Chem. Phys. 125, 144502.

van de Craats, A.M., Warman, J.M., Fechtenkötter, A., Brand, J.D., Harbison, M.A., Müllen, K., 1999. Record charge carrier mobility in a room-temperature discotic liquid-crystalline derivative of hexabenzocoronene. Adv. Mater. 11, 1469–1472.

van de Craats, A.M., Stutzmann, N., Bunk, O., Nielsen, M.M., Watson, M., Müllen, K., Chanzy, H.D., Sirringhaus, H., Friend, R.H., 2003. Meso-epitaxial solution-growth of self-organizing discotic liquid-crystalline semiconductors. Adv. Mater. 15, 495–499.

Watson, M.D., Fechtenkötter, A., Müllen, K., 2001. Big is beautiful-"aromaticity" revisited from the viewpoint of macromolecular and supramolecular benzene chemistry. Chem. Rev. 101, 1267–1300.

Wolfbeis, O.S., Koller, E., Hochmuth, P., 1985. The unusually strong effect of 4-cyano group upon electronic spectra and dissociation constants of 3-substituted 7-hydroxycoumarins. Bull. Chem. Soc. Jpn. 58, 731–734.

Yu, T.Z., Zhao, Y.L., Fan, D.W., 2006. Synthesis, crystal structure and photoluminescence of 3-(1-benzotriazole)-4-methyl-coumarin. J. Mol. Struct. 791, 18–22.

Yu, T.Z., Zhao, Y.L., Ding, X.S., Fan, D.W., Qian, L., Dong, W.K., 2007. Synthesis, crystal structure and photoluminescent behaviors of 3-(1H-benzotriazol-1-yl)-4-methyl-benzo[7,8]coumarin. J. Photochem. Photobiol. A: Chem. 188, 245–251.

Yu, T.Z., Zhang, P., Zhao, Y.L., Zhang, H., Meng, J., Fan, D.W., Chen, L.L., Qiu, Y.Q., 2010. Synthesis, crystal structure and photo- and electro-luminescence of the coumarin derivatives with benzotriazole moiety. Org. Electron. 11, 41–49.

Yu, T.Z., Zhu, Z.Y., Bao, Y.J., Zhao, Y.L., Liu, X.X., Zhang, H., 2017. Investigation of novel carbazole-functionalized coumarin derivatives as organic luminescent materials. Dyes Pigments 147, 260–269.

Zhang, Z.L., Jiang, X.Y., Zhu, W.Q., Zheng, X.Y., Wu, Y.Z., Xu, S.H., 2003. Blue and while emitting organic diodes based on anthracene derivative. Synth. Met. 137, 1141–1142.

Zhang, X., Xu, Z.Q., Si, W.L., Oniwa, K., Bao, M., Yamamoto, Y., Jin, T.N., 2017. Synthesis of extended polycyclic aromatic hydrocarbons by oxidative tandem spirocyclization and 1,2-aryl migration. Nat. Commun. 8, 15073.

Zhang, H., Yu, T.Z., Zhao, Y.L., Fan, D.W., Xi, Y.J., Zhang, P., 2010. Synthesis, crystal structure, photo- and electro-luminescence of 3-(4-(anthracen-10-yl)phenyl)-7-(N, N′-diethylamino)coumarin. Synth. Met. 160, 1642–1647.

Zhang, H., Luo, Q.L., Mao, Y.Z., Zhao, Y.L., Yu, T.Z., 2017. Synthesis and characterization of coumarin-biphenyl derivatives as organic luminescent materials. J. Photochem. Photobiol. A: Chem. 346, 10–16.

Zhang, H., Zhao, L., Luo, Q.L., Zhao, Y.L., Yu, T.Z., 2018. Synthesis, characterization and luminescent properties of anthracene- or pyrene-based coumarin derivatives. J. Fluoresc. 28, 1143–1150.